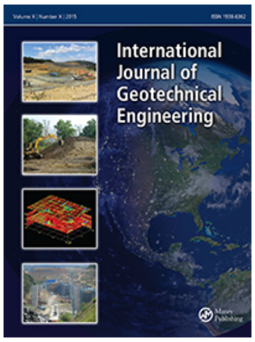

Taylor & Francis
Taylor & Francis Group

International Journal of Geotechnical Engineering

ISSN: 1938-6362 (Print) 1939-7879 (Online) Journal homepage: http://www.tandfonline.com/loi/yjge20

Prediction of vertical pile capacity of driven pile in cohesionless soil using artificial intelligence techniques

Ranajeet Mohanty, Shakti Suman & Sarat Kumar Das

To cite this article: Ranajeet Mohanty, Shakti Suman & Sarat Kumar Das (2016): Prediction of vertical pile capacity of driven pile in cohesionless soil using artificial intelligence techniques, International Journal of Geotechnical Engineering

To link to this article: http://dx.doi.org/10.1080/19386362.2016.1269043

Published online: 23 Dec 2016.

Prediction of vertical pile capacity of driven pile in cohesionless soil using artificial intelligence techniques

Ranajeet Mohanty, Shakti Suman and Sarat Kumar Das*

Piles are used in substructures of different infrastructural constructions. Due to the complex nature of soil, there are different empirical models to predict the bearing capacity of piles. The objective of the present study is to develop prediction models for vertical loaded driven piles in cohesionless soil using a novel artificial intelligence (AI) technique multi-objective genetic programming (MOGP). Two other recent AI techniques, multivariate adaptive regression spline (MARS) and functional network (FN), are also used to compare the efficacy of different AI techniques. The results MOGP, MARS and FN models are compared in terms of different statistical parameters such as correlation coefficient (R), absolute average error, root-mean–square-error, overfitting ratio and P_{50}. A ranking criteria approach has been implemented to assess the performance of the prediction models developed in this study along with other AI and empirical models available in the literature. The predictive model equations based on MOGP, MARS and FN are also presented.

Keywords: Pile, Vertical pile capacity, Artificial intelligence techniques, Multivariate adaptive regression splines, Functional network, Multi-objective genetic programming, Statistical performance

Introduction

Piles are commonly used for transferring the loads of superstructure to deeper depths. Interaction between the pile and the surrounding soil is highly ambiguous. As a result, a number of analytical and empirical methods have been proposed by different researchers for predicting the bearing capacity of piles. Some of these methods, which are commonly in use are presented in Das (2010). In spite of all the research, the mechanisms of pile foundations are not yet entirely understood. This has led to development of different empirical (statistical) methods which could include numerous factors that affect the pile load capacity.

Many researchers consider artificial intelligence (AI) technique as an alternate statistical tool. Compared to empirical methods, AI techniques are efficient in making predictions (Das and Basudhar 2006; Das *et al*. 2011; Muduli *et al*. 2013). Abu-Keifa (1998) used general regression neural network (GRNN) to model the vertical load-bearing capacity of driven piles in cohesionless soils. The GRNN contained three layers – one input layer, one hidden layer and one output layer. The developed GRNN model (Abu-Keifa 1998) was found to be better in comparison to empirical models as per American petroleum institute (RP2A 1984), Meyerhof (1976), Randolph (1985) and Coyle and Castello (1981). A data-set (4072 test samples) containing 17 input variables was used to develop prediction models of piles using back propagation neural network (BPNN) and MARS algorithm (Zhang and Goh 2016) and were found to be efficient. The MARS algorithm was found to be computationally more efficient in comparison with BPNN algorithm. Momeni *et al*. (2014) developed a hybrid model by combining artificial neural networks (ANN) with genetic algorithm (GA) for predicting the bearing capacity of piles. Similarly, other AI techniques also have been successfully implemented for predicting the ultimate bearing capacity of different types of piles using ANN (Das and Basudhar 2006; Lee and Lee 1996; Shahin *et al*. 2001; Tarawneh 2013; Teh *et al*. 1997), support vector machines (SVM) (Samui 2011), relevance vector machines (RVM) (Samui 2012a), multivariate adaptive regression splines (MARS) (Samui 2012b, Suman *et al*. 2016), extreme learning machines (ELM) (Muduli *et al*. 2013) and functional networks (FN) (Suman *et al*. 2016). Apart from load-bearing capacity of piles, ANN has also been used for predicting the settlement of piles based on cone penetration tests (CPT) (Baziar *et al*. 2015). But ANN has poor generalisation, attributed to attainment of local minima during training and needs iterative learning steps to obtain better learning performances.

Department of Civil Engineering, National Institute of Technology, Rourkela, Odisha 769008, India

*Corresponding author, email: sarat@nitrkl.ac.in

Received 1 September 2016; accepted 30 November 2016
DOI 10.1080/19386362.2016.1269043

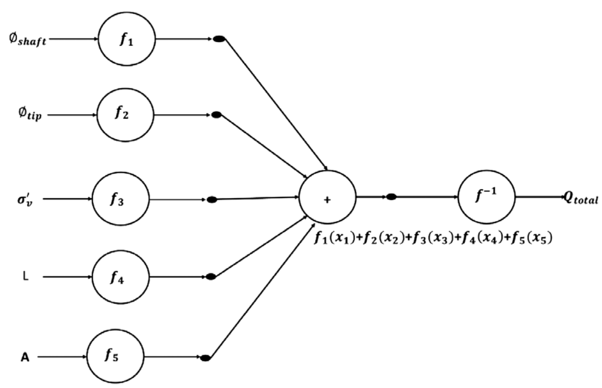

1 **Associative FN used in this study**

Hence, in recent times, MARS algorithm is being used for solving those types of problems, where the number of input variables is high. As a result, MARS is being increasingly used in many fields of science and economy (Lu *et al*. 2012; Cheng and Cao 2014). But its application to geotechnical engineering is very limited (Samui *et al*. 2011; Zhang and Goh 2016). Likewise, FN is also a recently developed technique. The structure of FN algorithm is related to the parameters of physical problems. It takes into consideration of both the knowledge of data-set and domain to create a relationship between the output parameter and the input parameters. Hence, application of FN in various research areas is increasing. Some of the areas where FN has been implemented with successes are: geotechnical engineering (Das and Suman 2015; Khan *et al*. 2016; Suman *et al*. 2016); structural engineering (Rajasekaran 2004); transportation engineering (Attoh-Okine 2005); petroleum engineering (El-Sebakhy *et al*. 2012); water resource engineering (Bruen and Yang 2005). Genetic programming (GP), which is an evolutionary algorithm, which is also called as 'grey box' method, is also in use (Muduli and Das 2014). The GP and its variant multi-gene genetic programming (MGGP) have been successfully implemented in the field of geotechnical engineering (Alavi and Gandomi 2011; Gandomi and Alavi 2012; Javadi *et al*. 2006; Muduli and Das 2014; Rezania and Javadi 2007; Yang *et al*. 2004). However, the most difficult part in implementation of GP or MGGP is a trade-off between the accuracy and complexity, controlling the maximum number of genes (G_{max}) and tree depth. With increase in G_{max}, the accuracy of the model is increased but at the same time complexity of the GP model increases, which may result in an overfitted model.

Hence, there is a need of mathematical framework for simultaneously increasing the accuracy and decreasing the complexity of the model. This can be achieved using multi-objective optimisation to simultaneously minimise the error function and complexity of the model. Recently, Gandomi *et al*. (2016) proposed multi-objective genetic programming (MOGP) to address this issue while discussing prediction model for concrete creep and found to be very efficient. Another advantage of this method is that the input parameters are selected in terms of complexity and root-mean-square error. Hence, the user can choose the suitable model. However, this has not been applied to any geotechnical engineering problems.

Hence, in the present study, an attempt has been made to use MOGP for determining the vertical capacity of driven piles in cohesionless soils. The results of MOGP have been compared with results of other AI techniques MARS and FN using different statistical criteria.

Methodology

A brief discussion about methodology of different AI techniques used in this study is presented as follows.

Multivariate adaptive regression splines (MARS)

MARS proposed by Friedman (1991) follows a non-linear, non-parametric approach. It creates relationships between different input variables by the help of coefficients and basis functions. MARS algorithm, follows a divide and conquer strategy. A MARS model contains a number of piece wise linear/cubic functions and knots (end points of splines). Creation of models in MARS follows a two-step process. In the first step, the basis functions which have the lowest training error are added sequentially. This process continues until the maximum number of basis function is reached. Then in the second step, the best viable submodel is obtained by removing the least effective terms. Once the pruning of model is complete, it is validated by generalised cross-validation (GCV) process. Elaborate discussion about MARS algorithm can be found in Das and Suman (2015), Samui *et al*. (2011) and Zhang and Goh (2016). For the sake of creating simple linear models, only piece-wise linear basis functions have been used in this study.

Functional network

Functional network (FN) proposed by Castillo *et al*. (2000) is an improvement over ANN. The advantage of FN over ANN is that it uses both the knowledge's of domain and data simultaneously. The initial topology of FN network is based on the domain knowledge of problem to be solved. Functional equations are used to simplify the preliminary topology of FN. Based on the learning method, functional networks are of two types viz. structural learning and parametric learning. In structural learning, preliminary topology of the network is built on the assets obtainable to the designer. Further simplification is undertaken with the help of functional equations. Whereas, in parametric learning, estimation of the neuron function is based on the combination of functional families and associated parameters are estimated from available data. A functional network is a combination of three types of units/elements. They are storing units (input layer, output layer and processing layers), computing units and directed link sets. The arrangement of the neural (node) functions $f_i(x)$ can be done as per the equation given below.

$$f_i(x) = \sum_{j=1}^{m} a_{ij}\phi_{ij}(X) \tag{1}$$

Where, ϕ is the shape function, having algebraic expressions, exponential functions and/or trigonometry functions. A set of linear or non-linear algebraic equations is obtained by the help of associative optimisation functions. This study applies the

Table 1 Statistics of driven piles used for modelling

	Maximum	Minimum	Mean	Standard deviation	Skewness
ϕ_{shaft} (°)	39.00	28.00	34.87	2.13	–0.28
ϕ_{tip} (°)	41.00	31.00	36.41	2.11	–0.09
σ_v'(kN/m^2)	475.00	38.00	179.80	82.39	1.00
L (m)	47.20	3.00	17.49	7.96	0.98
A (m^2)	0.66	0.01	0.13	0.10	2.68
$Q_{(m)}$ (kN)	5604.00	75.00	2207.63	1231.89	0.66

use of associative FNs and the schematic representation of the associative FN is presented in Fig. 1. Detailed discussions on FN can be found in Das and Suman (2015), Khan *et al*. (2016) and Suman *et al*. (2016).

Multi-objective genetic programming (MOGP)

GP is a subset of GA and is based on the principle of survival of the fittest. It is a combination of several GP trees. Each tree is composed of genes, which represents a lower non-linear transformation of input variables. When, the output is created from weighted linear combination of these genes it is termed as multi-gene genetic programming (MGGP). Unlike, conventional regression techniques GP or MGGP there are no need of predefined relationships for the problem.

In this research, a multi-objective genetic programming (MOGP) has been used. MOGP simultaneously optimises the complexity and error rate of the model. Complexity of the model can be calculated as the summation of all nodes including the sub-trees, whereas error rate used in this study is root-mean-square error (RMSE).

A typical minimisation of multi objective optimisation problem can be represented as: for a n dimensional decision variable, $x = \{x_1, x_2 \ldots\ldots, x_n\}$, find x^*, which minimises M objectives represented as $f(x^*) = \{f_1(x^*), f_2(x^*) \ldots\ldots, f_M(x^*)\}$, subject to a set of constraints $h_i(x^*) = 0$; $j = 1, \ldots p$. These objectives are conflicting in nature. So, minimising x corresponding to a single objective will result in an unacceptable solution for other objectives. Hence, perfectly minimising all the objectives simultaneously is nearly impossible. Therefore, finding a set of optimal solutions, which is within the accepted level of each objective without being dominated by other solutions, is the preferred way to multi objective optimisation technique. It produces a Pareto front from which a user can find a trade-off solution between conflicting objectives. Pareto front is defined as the set of non-dominated solutions, where each objective is considered as equally important. A feasible solution x dominates other feasible solution y, only when $f_i(x) \leq f_i(y)$ for $i = 1, \ldots M$ and $f_j(x) < f_j(y)$ for at least one objective function j. Therefore, while comparing with two feasible solutions, three types of dominance can exist and they are:

- y is dominated by x
- x is dominated by y
- both x and y are non-dominated to each other

In this research GPTIPS 2 developed by Searson (2015) was used for model development. For multi-objective optimisation, non-dominated sorting technique of Deb *et al*. (2002) was used. The non-dominated sorting was implemented at the end of each generation to produce a set of Pareto optimal solutions.

Database and pre-processing

For the development of prediction models for vertical capacity of piles, data-set of Abu-Keifa (1998) has been used in this study. The database consists of in-situs test on soil and pile load test data from different parts of the world. The database includes angle of shear resistance of soil at the shaft (ϕ_{shaft}) and at the tip (ϕ_{tip}) of the pile, effective overburden pressure (σ_v') at the tip of the pile, length of pile (L) and cross-sectional area of pile (A) and are considered here as inputs along with total pile capacity ($Q_{(m)}$), which is considered as output. Statistics of soil and pile load data used in this study is presented in Table 1. The data-set was randomly divided into training (50 data samples) and testing (9 data samples). For MARS and FN analysis, data were normalised in the range [0, 1] and in MOGP, data normalisation is not required. However, following MOGP parameters are considered, population size 500, number of generations 100, tournament size 50, mutation rate 10%, crossover rate 85% and reproduction rate was 5%.

Results and discussions

Three different prediction models were developed for driven piles using MOGP, MARS and FN, algorithm. Statistical performance of the developed models was found in terms of correlation coefficient (R), average absolute error (AAE), root-mean-square error (RMSE) overfitting ratio (ratio between the RMSE of testing to training) and cumulative probability distribution of $Q_{(p)}/Q_{(m)}$) i.e. P_{50}. Overfitting ratio indicates the generalisation of the prediction models and models having P_{50} value closer to 1.0 are considered to be more efficient in predictions, more than 1.0 is over prediction and less than 1.0 is under prediction. Based on various statistical criteria, different models may perform differently. Therefore, a ranking index method as proposed by Abu-Farsakh and Titi (2004) is implemented to measure the overall performance of the prediction models taking into account different performance criteria. Four different evaluation (ranking) criteria were considered in this study. First, ranking (best fit calculations) criterion represented as $R1$, consists of correlation coefficient (R) and Nash-Sutcliff coefficient of efficiency (E). Since coefficient of determination (R^2) is a biased estimate, therefore E was considered in place of R^2 (Das 2013). A value closer to one for R and E indicates a better model. Second ranking criterion $R2$ (arithmetic calculations) consists of arithmetic mean (μ) and standard deviation (σ) of the $Q_{(p)}/Q_{(m)}$ ratio ($Q_{(p)}$ = predicted pile capacity; $Q_{(m)}$ = measured pile capacity). The most optimum performance is observed, when μ is closer to one and σ is closer to zero. The third ranking criterion $R3$ (cumulative probability distribution of $Q_{(p)}/Q_{(m)}$) contains the P_{50} and P_{90} values of $Q_{(p)}/Q_{(m)}$. In this case model having P_{50} value closer to one and least difference between the P_{90} and P_{50} value is considered to be most efficient. And finally the fourth ranking criterion $R4$ contains the histogram and log-normal distribution of $Q_{(p)}/Q_{(m)}$. The maximum variation of the prediction from the actual value was taken as 20%. Combining all the four ranking criteria, a ranking index

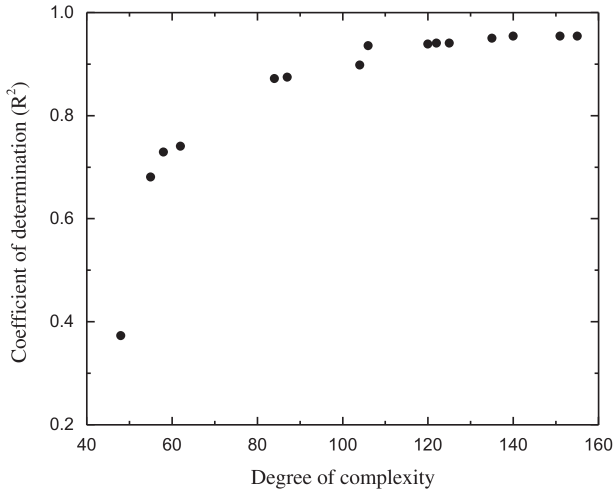

2 Degree of complexity vs. R^2

Table 2 Statistical performance of AI models for driven piles

		R	AAE (kN)	RMSE (kN)	Over-fitting ratio	P_{50}
MARS	Training	0.966	244.61	310.87	1.135	0.998
	Testing	0.970	308.56	352.93		
FN	Training	0.962	227.02	334.05	1.048	1.000
	Testing	0.960	295.01	350.15		
MOGP	Training	0.970	223.09	302.88	0.885	1.000
	Testing	0.986	234.45	267.93		

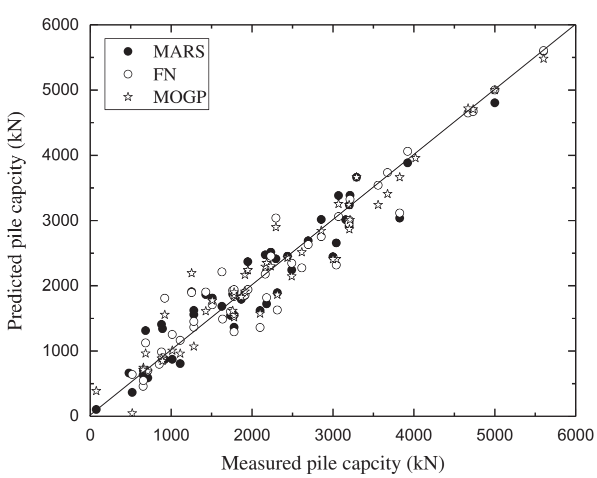

3 Plot of measured and predicted load-bearing capacity of driven piles for training data-set

(RI) was obtained and all the models were given an overall rank (lower RI means better the rank of the model). Details of the ranking system can be found in Abu-Farsakh and Titi (2004), Muduli *et al*. (2013).

MOGP Model

From the analysis the Pareto optimal front, indicating the complexity of the model against the coefficient of determination (R^2) is presented in Fig. 2. From Fig. 2, it can be observed that as degree of complexity of model increases R^2 also increases and becomes constant. Thus, the chosen optimal model had a degree of complexity as 104 and R^2 as 0.936. Model equation for load-bearing capacity of pile is presented below as per Equation (2).

$$\begin{aligned} Q_{(p)} &= 719\tan(LA^2) - 521L - 1466\phi_{shaft} + 521\ln\left\{\ln(\sigma'_v)\right\} \\ &-449\sin\left\{\sin(\phi^3_{shaft})\right\} + 0.0728e^{\tan\{\tan(\phi_{tip})\}} \\ &+226L + 0.848\tan(\phi_{tip}) + 25.2\sigma'_v\ln\left\{\ln(\phi_{shaft})\right\} \\ &-3.47\sigma_v'^{3A^{2\ln\{\ln\{\phi_{tip})\}}} + 1466L^{\tan(A)} + 0.422\phi^3_{shaft} + 31100 \end{aligned} \tag{2}$$

As per Table 2, the values of R in training and testing for MOGP model are 0.970 and 0.986, respectively. The AAE and RMSE values for training and testing of MOGP model are 223.09, 302.88 and 234.45, 267.93 kN, respectively (Table 2). The overfitting ratio (Table 2) of MOGP model is 0.885, which indicates that the predicted model is not well generalised. But the P_{50} value of MOGP model is 1.000, which indicates that the developed model is good in predictions. In training stage for capacities of piles less than 3000 kN, the MOGP model gives equal predictions around the line of equality (Fig. 3) and for capacity of piles greater than 3000 kN, it mostly gives under predictions. During testing (Fig. 4), when load-bearing capacity of driven piles is less than 1500 kN, the MOGP model gives under predicted values. However, when capacity of piles is greater than 1500 kN then it over predicts. Also the cumulative probability distribution of the MGGP model is presented in Fig. 5.

The AAE and RMSE values, MOGP model, have least error for both training and testing. Also the P_{50} value of FN and MOGP model is exactly 1. The advantage of MOGP is that it produces compact non-linear mathematical models in comparison with MARS and FN. Also data normalisation in case of MOGP is unnecessary.

MARS Model

The maximum number of BFs influences the accuracy and complexity of the MARS model. With increase in the number of BFs, both accuracy and complexity of the model increase, whereas, both accuracy and complexity of the model decrease with a decrease in the number of BFs. Therefore, an optimal number of BFs should be chosen so that the developed model is simple and at the same time is also highly accurate. In this paper by the help of trial and error method, the optimal number of BFs for MARS model was found to be 10 and its corresponding equation for predicting the vertical capacity of piles is presented below.

$$\begin{aligned} Q_{(p)} = \; &-56.59 + 7956.231BF1 - 6502.104BF2 \\ &+15663.657BF3 - 27390.666BF4 - 13098.201BF5 \\ &+16664.406BF6 - 2001702.573BF7 + 66187.659BF8 \\ &-110801.16BF9 - 1151558.004BF10 \end{aligned} \tag{3}$$

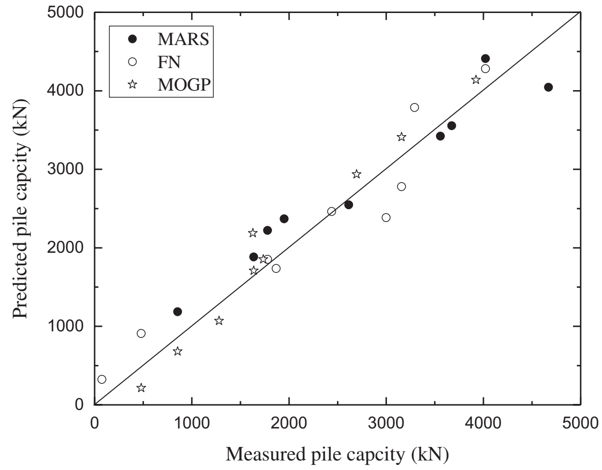

4 Plot of measured and predicted load-bearing capacity of driven piles for testing data-set

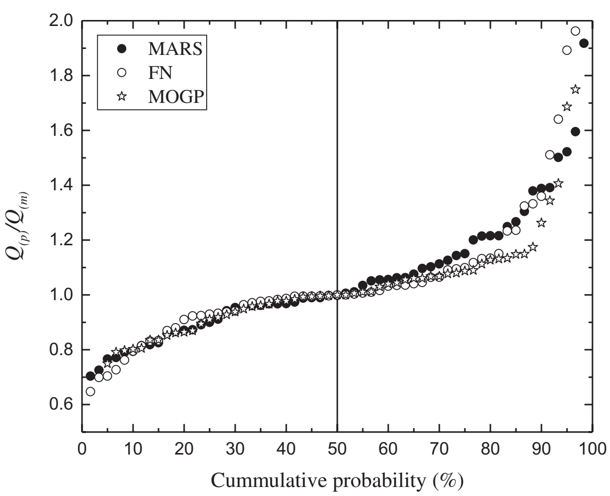

5 Cumulative probability distribution of the prediction models

Table 3 BFs for the MARS model to predict load-bearing capacity of driven piles

***BF*1**	***max*(0, *A*-0.245)**	***BF*6**	***max*(0, 0.47-*L*)**
*BF*2	*max*(0, 0.245-*A*)	*BF*7	*BF*6 *max*(0, σ_v'-0.423)
*BF*3	*max*(0, σ_v'-0.22)	*BF*8	*max*(0, 0.47-*L*) *max*(0, 0.423-σ_v') *max*(0, ϕ_{tip}-0.65)
*BF*4	*max*(0, 0.22-σ_v')	*BF*9	*BF*1 *max*(0, 0.38-*L*)
*BF*5	*max*(0, *L*-0.47)	*BF*10	*BF*3 *max*(0, 0.275-σ_v')

The BFs used in Equation (3) are given in the Table 3. Figs. 3 and 4 show the plot between measured and predicted bearing capacities of driven piles for training and testing, respectively. For training data for capacities of piles less than 3000 kN, the MARS model gives good predictions around the line of equality (Fig. 3). But, for pile capacity greater than 3000 kN, it mostly gives under predicted values. While, with testing data (Fig. 4), when load-bearing capacity of driven piles is less than 2500 kN, then MARS model gives over predicted values. However, when capacity of piles is greater than 2500 kN then it mostly under predicts the values. As per Table 2, the values of *R* in training and testing for MARS model are 0.966 and 0.970, respectively, indicating a strong correlation according to Smith (1986). The AAE and RMSE values for training and testing of MARS model are 244.61, 310.87 kN and 308.56, 352.93 kN, respectively, (Table 2). The overfitting ratio of MARS model is 1.135, which indicates that the generalisation of the predicted model is not very efficient. The P_{50} value of MARS model is 0.998, which indicates that the developed model is good in predictions. Also the cumulative probability distribution of the MARS model is presented in Fig. 5.

FN model

For the sake of simplicity, a FN model with exponential BF and degree 5 was adopted in this study. The corresponding FN model equation is given by Equation (4).

$$
\begin{aligned}
Q_{(p)} = \; & -4485.866 - 66905.158e^{2\phi_{shaft}} + 300746.275e^{3\phi_{shaft}} \\
& -431369.056e^{4\phi_{shaft}} + 198441.433e^{5\phi_{shaft}} \\
& -55095.937e^{2\phi_{tip}} + 183832.556e^{3\phi_{tip}} - 212370.225e^{4\phi_{tip}} \\
& +82732.159e^{5\phi_{tip}} + 13026.848e^{\sigma_v'} + 193250.278e^{3\sigma_v'} \\
& -638850.695e^{4\sigma_v'} + 496989.347e^{5\sigma_v'} - 338527.562e^{3L} \\
& +927906.317e^{4L} - 651475.038e^{5L} + 60835.66e^{2A} \\
& -149164.367e^{3A} + 91299.288e^{4A}
\end{aligned} \tag{4}
$$

The values of the inputs to be entered in Equation 4 should be normalised in the range [0, 1]. The *R* values for FN model in training and testing are 0.962 and 0.960, respectively, (Table 2). These values suggest a strong correlation (Smith 1986). The AAE and RMSE values for training and testing of FN model are 227.02, 334.05 kN and 295.01, 350.15 kN, respectively, (Table 2). The overfitting ratio (Table 2) of FN model is 1.048, which indicates that the predicted model is well generalised. Also the P_{50} value of FN model is 1.000, which indicates that the developed model is good in predictions. In training stage for capacities of piles less than 3000 kN, the FN model gives equal predictions around the line of equality (Fig. 3). And for capacity of piles greater than 3000 kN, it gives cent per cent accurate predictions. During testing (Fig. 4), when load-bearing capacity of driven piles is less than 2500 kN, then FN model gives mostly over-predicted values. However, when capacity of piles is greater than 2500 kN than it gives equal distributions. The overfitting ratio of FN model is much closer to unity in comparison with other models. Also the cumulative probability distribution of the FN model is presented in Fig. 5.

Comparison of models

According to the first ranking criteria (*R*1) GRNN model (Abu-Keifa 1998) is ranked 1 (*R*1 = 1) as both the *R* and *E* were much closer to one as compared to other AI models (Table 4). It is trailed by MOGP model (*R*1 = 2), which is followed by MARS having *R*1 = 3. The least efficient model is Meyerhof (1976) model with *R*1 = 6. In the second ranking criteria *R*2, MARS model comes first (*R*2 = 1) followed by FN model

Table 4 Ranking of various models for driven piles based on ranking index

	Best fit calculations			Arithmetic calculations of $Q_{u(p)}/Q_{u(m)}$			Cumulative probability of $Q_{u(p)}/Q_{u(m)}$			±20% Accuracy (%)			Overall rank	
	R	*E*	*R*1	*μ*	*σ*	*R*2	P_{50}	P_{90}	*R*3	Log-normal	Histogram	*R*4	RI	Final rank
MARS	0.966	0.932	3	1.056	0.230	1	0.998	1.388	4	67	66	1	9	1
FN	0.961	0.924	4	1.100	0.492	2	1.000	1.360	2	52	73	3	11	3
MOGP	0.970	0.941	2	1.073	0.590	3	1.000	1.262	1	36	81	4	10	2
GRNN (Abu-Keifa 1998)	0.974	0.947	1	1.139	0.800	4	1.002	1.290	3	49	81	2	10	2
Meyerhof (1976)	0.738	−6.362	6	1.762	0.856	6	1.697	3.124	6	21	25	5	23	5
Coyle and Castello (1981)	0.767	−0.179	5	0.523	0.347	5	0.426	1.036	5	11	10	6	21	4

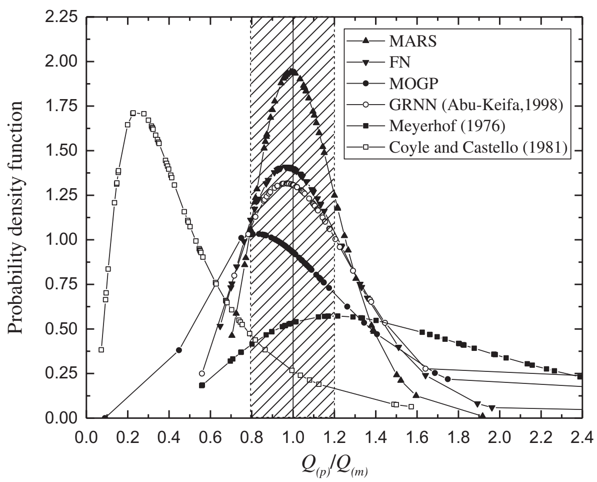

6 Log-normal distribution of $Q_{(p)}/Q_{(m)}$ for different AI models

(*R*2 = 2). The last two models are Coyle and Castello (1981) model (*R*2 = 5) and Meyerhof (1976) model (*R*2 = 6). For the third ranking criteria *R*3, MOGP model is ranked 1 (*R*3 = 1) followed by FN model with *R*3 = 2. It is trailed by GRNN model (Abu-Keifa 1998) with *R*3 = 3 and MARS model *R*3 = 4. Based on *R*4 (fourth ranking criteria), MARS model leads the pack with *R*4 = 1. It is followed by GRNN model (Abu-Keifa 1998) (*R*4 = 2). The last two models are Meyerhof (1976) model (*R*4 = 5) and Coyle and Castello (1981) model (*R*4 = 6). The log-normal distribution of $Q_{(p)}/Q_{(m)}$ of different AI models is presented in Fig. 6. As per Table 4 in the overall ranking system, MARS model is ranked 1 with a RI value of 9. The second spot is jointly shared by MOGP and GRNN model (Abu-Keifa 1998) (RI = 10), which is succeeded by FN model having rank 3 (RI = 11). And finally the last two ranked models are Coyle and Castello (1981) having rank 4 (RI = 21) and Meyerhof (1976) model having rank 5 (RI = 23).

However, it should be kept in mind that the GRNN model is not comprehensive (59 hidden neurons) as compared to the AI models developed in this study. Also the performance of the AI models developed in this study is somewhat comparable to the GRNN model. It can be argued here that the error values for MARS, FN and MOGP models are marginally more than those for the GRNN model, but the mathematical models given by MARS, FN and MOGP are comprehensive and most suited to be used by a practicing geotechnical engineer. Thus, the simplicity of understanding at the cost of minimal loss of accuracy should make MARS, FN and MOGP models, a favourable choice for field applications. Whereas in comparison with AI models, performance of empirical models is poor as indicated in Table 4.

Conclusions

The present study discussed about the application of multi-objective genetic programming (MOGP), multivariate adaptive regression splines (MARS) and functional network (FN) to predict the vertical load capacity of driven piles in cohesionless soils. The results of the present study and results obtained previously in the literature were compared in terms of various statistical parameters. From the results, MOGP model was found to be better in terms of correlation coefficient (*R*), absolute average error (AAE) and root-mean-square error (RMSE); FN model was better in terms of overfitting ratio; and FN and MOGP model were better in terms of P_{50} value (P_{50} = 1.000). As per the ranking method, MARS model was ranked 1, GRNN and MOGP models were both ranked 2 and finally FN model was ranked 3. But, it should be noted that the GRNN model as available in the literature is not comprehensive. Whereas the AI models developed in this paper are simple and fairly accurate in comparison to GRNN.

Disclosure statement

No potential conflict of interest was reported by the authors.

ORCID

Ranajeet Mohanty http://orcid.org/0000-0001-9837-9140

References

Abu-Farsakh, M. Y. and Titi, H. H. 2004. Assessment of direct cone penetration test methods for predicting the ultimate capacity of friction driven piles, *Journal of Geotechnical and Geoenvironmental Engineering*, **130**, (9), 935–944.

Abu-Kiefa, M. A. 1998. General regression neural networks for driven piles in cohesionless soils, *Journal of Geotechnical and Geoenvironmental Engineering* ASCE, **124**, (12), 1177–1185.

Hossein Alavi, A. H. and Hossein Gandomi, A. H. 2011. A robust data mining approach for formulation of geotechnical engineering systems, *Engineering with Computers*, **28**, (3), 242–274.

Attoh-Okine, N. O. 2005. Modeling incremental pavement roughness using functional network, *Canadian Journal of Civil Engineering*, **32**, (5), 899–905.

Baziar, M. H., Azizkandi, A. S. and Kashkooli, A. 2015. Prediction of pile settlement based on cone penetration test results: An ANN approach, *KSCE Journal of Civil Engineering*, **19**, (1), 98–106.

Bruen, M. and Yang, J. 2005. Functional networks in real-time flood forecasting—a novel application, *Advances in Water Resources*, **28**, (9), 899–909.

Castillo, E., Cobo, A., Gomez-Nesterkin, R. and Hadi, A. S. 2000. A general framework for functional networks, *Networks*, **35**, (1), 70–82.

Cheng, M. Y. and Cao, M. T. 2014. Accurately predicting building energy performance using evolutionary multivariate adaptive regression splines, *Applied Soft Computing*, **22**, 178–188.

Coyle, H. M. and Castello, R. R. 1981. New design correlations for piles in sand, *Journal of Geotechnical Engineering*, ASCE, **107**, (7), 965–986.

Das, B. M. 2010. Principles of foundation engineering. 7th ed, Stamford, CT, CL-Engineering.

Das, S. K. and Basudhar, P. K. 2006. Undrained lateral load capacity of piles in clay using artificial neural network, *Computers and Geotechnics*, **33**, (8), 454–459.

Das, S. K. and Suman, S. 2015. Prediction of lateral load capacity of pile in clay using multivariate adaptive regression spline and functional network, *Arabian Journal for Science and Engineering*, **40**, (6), 1565–1578.

Das, S. K. 2013. Artificial neural networks in geotechnical engineering: modeling and application issues chapter 10, in Metaheuristics in water, geotechnical and transport engineering, (eds. X. Yang, A. H. Gandomi, S. Talatahari, A. H. Alavi), 231–270, London, Elsevier.

Das, S. K., Biswal, R. K., Sivakugan, N. and Das, B. 2011. Classification of slopes and prediction of factor of safety using differential evolution neural networks, *Environmental Earth Sciences*, **64**, (1), 201–210.

Deb, K., Pratap, A., Agarwal, S. and Meyarivan, T. 2002. A fast and elitist multiobjective genetic algorithm: NSGA-II, *IEEE Transactions on Evolutionary Computation*, **6**, (2), 182–197.

El-Sebakhy, E. A., Asparouhov, O., Abdulraheem, A. A., Al-Majed, A. A., Wu, D., Latinski, K. and Raharja, I. 2012. Functional networks as a new data mining predictive paradigm to predict permeability in a carbonate reservoir, *Expert Systems with Applications*, **39**, (12), 10359–10375.

Friedman, J. 1991. Multivariate adaptive regression splines, *Annals of Statistics*, **19**, 1–67.

Gandomi, A. H. and Alavi, A. H. 2012. A new multi-gene genetic programming approach to non-linear system modeling. Part II: geotechnical and earthquake engineering problems, *Neural Computing and Applications*, **21**, (1), 189–201.

Gandomi, A. H., Sajedi, S., Kiani, B. and Huang, Q. 2016. Genetic programming for experimental big data mining: A case study on concrete creep formulation, *Automation in Construction*, **70**, 89–97.

Javadi, A. A., Rezania, M. and Nezhad, M. M. 2006. Evaluation of liquefaction induced lateral displacements using genetic programming, *Computers and Geotechnics*, **33**, (4–5), 222–233.

Khan, S. Z., Suman, S., Pavani, M. and Das, S. K. 2016. Prediction of the residual strength of clay using functional networks, *Geoscience Frontiers*, **7**, (1), 67–74.

Lee, I. M. and Lee, J. H. 1996. Prediction of pile bearing capacity using artificial neural networks, *Computers and Geotechnics*, **18**, (3), 189–200.

Lu, C. J., Lee, T. S. and Lian, C. M. 2012. Sales forecasting for computer wholesalers: A comparison of multivariate adaptive regression splines and artificial neural networks, *Decision Support Systems*, **54**, (1), 584–596.

Meyerhof, G. G. 1976. Bearing capacity and settlement of pile foundations, *Journal of Geotechnical Engineering*, ASCE, **102**, (3), 196–228.

Momeni, E., Nazir, R., Armaghani, D. J. and Maizir, H. 2014. Prediction of pile bearing capacity using a hybrid genetic algorithm-based ANN, *Measurement*, **57**, 122–131.

Muduli, P. and Das, S. 2014. Evaluation of liquefaction potential of soil based on standard penetration test using multi-gene genetic programming model, *Acta Geophysica*, **62**, (3), 529–543.

Muduli, P. K., Das, S. K. and Das, M. R. 2013. Prediction of lateral load capacity of piles using extreme learning machine, *International Journal of Geotechnical Engineering*, **7**, (4), 388–394.

Rajasekaran, S. 2004. Functional Networks in Structural Engineering, *Journal of Computing in Civil Engineering*, **18**, (2), 172–181.

Randolph, M. F. 1985. Capacity of piles driven into dense sand, Rep. Soils TR I7I, Engrg. Dept., Cambridge University, Cambridge, UK.

Rezania, M. and Javadi, A. A. 2007. A new genetic programming model for predicting settlement of shallow foundations, *Canadian Geotechnical Journal*, **44**, (12), 1462–1473.

RP2A. 1984. Recommended practice for planning, designing and constructing fixed offshore platfonns, 15th (ed.), American Petroleum Institute, Washington, DC.

Samui, P. 2011. Prediction of pile bearing capacity using support vector machine, *International Journal of Geotechnical Engineering*, **5**, (1), 95–102.

Samui, P. 2012a. Application of relevance vector machine for prediction of ultimate capacity of driven piles in cohesionless soils, *Geotechnical and Geological Engineering*, **30**, (5), 1261–1270.

Samui, P. 2012b. Determination of ultimate capacity of driven piles in cohesionless soil: A Multivariate Adaptive Regression Spline approach, *International Journal for Numerical and Analytical Methods in Geomechanics*, **36**, (11), 1434–1439.

Samui, P., Das, S. and Kim, D. 2011. Uplift capacity of suction caisson in clay using multivariate adaptive regression spline, *Ocean Engineering*, **38**, (17–18), 2123–2127.

Searson, D. P. 2015. GPTIPS 2: an open-source software platform for symbolic data mining, in Handbook of genetic programming applications, 551–573, Springer International Publishing, New York.

Shahin, M. A., Jaksa, M. B. and Maier, H. R. 2001. Artificial neural network applications in geotechnical engineering, *Australian Geomechanics*, **36**, (1), 49–62.

Smith, G. N. 1986. Probability and statistics in civil engineering: An introduction, London, Collins.

Suman, S., Das, S. K. and Mohanty, R. 2016. Prediction of friction capacity of driven piles in clay using artificial intelligence techniques, *International Journal of Geotechnical Engineering*, **10**, (5), 1–7.

Tarawneh, B. 2013. Pipe pile setup: Database and prediction model using artificial neural network, *Soils and Foundations*, **53**, (4), 607–615.

Teh, C. I., Wong, K. S., Goh, A. T. C. and Jaritngam, S. 1997. Prediction of pile capacity using neural networks, *Journal of Computing in Civil Engineering*, ASCE, **11**, (2), 129–138.

Yang, C. X., Tham, L. G., Feng, X. T., Wang, Y. J. and Lee, P. K. 2004. Two-stepped evolutionary algorithm and its application to stability analysis of slopes, *Journal of Computing in Civil Engineering*, ASCE, **18**, (2), 145–153.

Zhang, W. and Goh, A. T. C. 2016. Multivariate adaptive regression splines and neural network models for prediction of pile drivability, *Geoscience Frontiers*, **7**, (1), 45–52.

Appendix 1.

Data-set used in the present study

$\varphi_{(shaft)}$	$\varphi_{(tip)}$	σ'_v (kN/m²)	L(m)	A(m²)	$Q_{m(total)}$(kN)	Site
33	38	255	24.5	0.131	2615	Low-Sill Structure, Old River
34	37.5	206	19.8	0.223	3674	Low-Sill Structure, Old River
33	38	223	21.5	0.131	2164	Low-Sill Structure, Old River
33	37.5	210	20.2	0.1468	3042	Low-Sill Structure, Old River
33	37	206	19.9	0.1821	2856	Low-Sill Structure, Old River
38	41	138	11.6	0.209	3558	Lonesville, La.
38	40	164	13.7	0.209	3292	Lonesville, La.
38	40	196	16.5	0.209	3923	Lonesville, La.
35	37	158	16.2	0.105	1637	Arkansas River Project LD4
35	37	158	16.1	0.1644	2233	Arkansas River Project LD5
35	36.5	158	16.2	0.2109	2295	Arkansas River Project LD6
36.5	36.5	120	12.3	0.1654	1779	Arkansas River Project LD7
34	38	475	47.2	0.2917	5604	Low Arrow Lake, B.C., Canada
34	34	38	3	0.1644	712	Ogeeches River, Ga.
35	35	72	6.1	0.1644	1735	Ogeeches River, Ga.
35	35	100	8.9	0.1644	2491	Ogeeches River, Ga.
36	36	131	12	0.1644	3158	Ogeeches River, Ga.
36	36	161	15	0.1644	3825	Ogeeches River, Ga.
35.5	36	163	15.2	0.1301	2695	Ogeeches River, Ga.
34	38	146	11.3	0.0316	1429	Tokyo, Japan
35.5	35.5	89	9.1	0.0864	658	St. Charles River, Que., Canada
35.5	35.5	119	12.2	0.0864	882	St. Charles River, Que., Canada
35.5	35.5	148	15.2	0.0864	1014	St. Charles River, Que., Canada
35.5	35.5	178	18.3	0.0864	1281	St. Charles River, Que., Canada
35.5	35.5	89	9.1	0.0799	655	St. Charles River, Que., Canada
35.5	35.5	119	12.2	0.0799	894	St. Charles River, Que., Canada
35.5	35.5	148	15.2	0.0799	1113	St. Charles River, Que., Canada
35.5	35.5	178	18.3	0.0799	1281	St. Charles River, Que., Canada
31	31	134	16	0.0613	480	Holemen Island, Drammen, Norway
31	31	134	16	0.0316	519	Holemen Island, Drammen, Norway
33	33	111	12.2	0.0061	75	Albysjon, Sweden
39	39.5	75	7	0.0999	2439	North Sea, The Netherlands
39	39.5	72	6.7	0.0999	3000	North Sea, The Netherlands
39	39.5	56	5.2	0.0999	1950	North Sea, The Netherlands
32	34	198	21	0.2313	3200	Zeebrugge, Belgium
37.5	40	301	29.9	0.3075	4733	West Seattle Freeway
37.5	39.5	258	25.6	0.3075	4021	West Seattle Freeway
33	35	169	18	0.6568	5000	Gadiz, Spain
28	39	213	16.8	0.1431	4670	Tacoma, Wash.
34	35	111	12.2	0.1143	854	Clyde VaHey-Glasgow, Scotland
32	35	241	23.3	0.1486	1628	Clyde VaHey-Glasgow, Scotland
34	35	92	9.1	0.1291	685	Clyde VaHey-Glasgow, Scotland
32	37	176	17.5	0.3855	3069	Biograd Yugoslavia
35	37	246	23.8	0.0729	1913	Missouri
35	37	183	17.7	0.0729	2313	Missouri
35	37	260	25.3	0.0729	1254	Connecticut
39	39.5	56	5.2	0.0999	1948	North Sea, The Netherlands
33	35.5	343	34.1	0.0325	1761	Cohasset, Minn.
34	36	319	31.7	0.0325	2180	Cohasset, Minn.
33	33	335	29.3	0.0557	3203	Kaohsiung, China
33	34	354	31.1	0.0557	3211	Kaohsiung, China
36	37	215	21.3	0.0409	1779	Winnemucca, Nev.
36	37	209	20.7	0.0827	1868	Winnemucca, Nev.
35	35	242	24.1	0.066	1779	Winnemucca, Nev.
36	37	209	20.7	0.0929	1913	Winnemucca, Nev.
35	35	166	16.5	0.0613	2100	Winnemucca, Nev.
35	35	178	17.7	0.0827	1509	Winnemucca, Nev.
35.5	37	228	21.9	0.066	922	Winnemucca, Nev.
35	35	178	17.7	0.0929	1779	Winnemucca, Nev.